Progress In Electromagnetics Research M, Vol. 64, 157–166, 2018

Modeling of Dispersive Chiral Media Using the ADE-TLM Method

Khalid Mounirh*, Soufiane El Adraoui, Yasser Ekdiha, Mohamed I. Yaich, and Mohsine Khalladi

Abstract—In this paper, an efficient Transmission Line Matrix (TLM) algorithm for modeling chiral media is presented. The formulation is based on auxiliary differential equations (ADE) of electric and magnetic current densities. Permittivity and permeability are assumed to follow the Lorentz model while chirality is assumed to follow the Condon model. The proposed method models the dispersive nature of permittivity, permeability, and chirality by adding both voltage and current sources in supplementary stubs to the conventional symmetrical condensed node (SCN) of the TLM method. The electromagnetic coupling appears explicitly in the update equations of the voltage and current sources. The algorithm is developed to simulate electromagnetic wave propagation in a chiral medium. The co-polarized and cross-polarized transmitted and reflected waves from a chiral slab due to a normal incident plane wave are calculated. Validation is performed by comparing the results obtained from the proposed method with those obtained analytically.

1. INTRODUCTION

Chiral materials have attracted great interest and inspired many theoretical and experimental investigations and applications. They are still ideal candidates for future microwave devices and structures due to their unique properties. Among the main interesting properties, we find optical activity (OA), a property that reflects the ability of the medium to rotate the polarization plane of the incident wave. The variation of optical activity as a function of frequency determines another important property known as optical rotatory dispersion (ORD). Chiral materials are also characterized by an absorption divergence depending on whether the circular polarization is right or left, the property known as circular dichroism (CD). In virtue of these properties, chiral mediums are classified as materials having a magnetoelectric coupling and find various applications in circular polarizers [1], microstrip substrates [2], cloaking devices [3], absorbers [4], antennas radomes [5], antenna arrays [6] and waveguides [7].

Electromagnetic waves interaction with chiral medium is an important problem that has been widely studied analytically and numerically. Several studies have dealt with the modeling of biisotropic and chiral media by using the FDTD method. These studies, based on various assumptions of constitutive relations, have proposed several modeling techniques. Among these techniques we find the modulation of the Yee cell, presented by Grande et al. [8], as well as the decomposition of electric and magnetic fields presented by Akyurtlu et al. [9–13]. The first rigorous formulation that gave a complete model was obtained by incorporating the dispersive nature of the constituent parameters of the studied media [14]. In this model, the frequency dependence of permeability and permittivity was presented by the Lorentz model while chirality was presented by the Condon model. These models of frequency dependencies were subsequently used with other techniques in several publications [15–19]. These techniques include: z transform [15], Shift-Operator [16], auxiliary differential equations [17, 18], and Mobius transformation [19].

Received 1 November 2017, Accepted 18 January 2018, Scheduled 9 February 2018

* Corresponding author: Khalid Mounirh (khalidmounirh@gmail.com).

The authors are with the EMG Group, LaSIT Laboratory, Abdelmalek Essaadi University, Tetouan, Morocco.

On the other hand, in the literature, few publications have dealt with the TLM modeling of chiral media. We find the use of the Z-transform technique by Paul et al. [20], the use of constant recursive convolution (CRC) technique with the SCN by Yaich et al. [21] and the use of analogies between field and circuit parameters with the technique of adding voltage sources by Cabeceira et al. [22].

2. FORMULATIONS AND EQUATIONS

In the case of a chiral medium, Maxwell's curl equations in time-harmonic forms are given by [23]:

$$\boldsymbol{\nabla} \times \mathbf{E} = -j\omega\mu(\omega)\,\mathbf{H} + \frac{\omega}{c_0}\kappa(\omega)\mathbf{E} \tag{1a}$$

$$\boldsymbol{\nabla} \times \mathbf{H} = j\omega\varepsilon(\omega)\,\mathbf{E} + \frac{\omega}{c_0}\kappa(\omega)\mathbf{H} \tag{1b}$$

where c_0 is the speed of light, and ε, μ, and κ are respectively the permittivity, permeability and chirality coefficients. The expressions of these parameters are given by the Lorentz model for ε and μ and by the Condon model for κ:

$$\varepsilon(\omega) = \varepsilon_0\left(\varepsilon_\infty + \frac{(\varepsilon_s - \varepsilon_\infty)\,\omega_e^2}{\omega_e^2 + j2\delta_e\omega - \omega^2}\right) \tag{2a}$$

$$\mu(\omega) = \mu_0\left(\mu_\infty + \frac{(\mu_s - \mu_\infty)\,\omega_h^2}{\omega_h^2 + j2\delta_h\omega - \omega^2}\right) \tag{2b}$$

$$\kappa(\omega) = \frac{\tau_\kappa\,\omega_\kappa^2\,\omega}{\omega_\kappa^2 + j2\delta_\kappa\omega_\kappa\omega - \omega^2} \tag{2c}$$

where ε_∞ and μ_∞ are the relative permittivity and relative permeability at infinite frequency; ε_s and μ_s are the relative permittivity and relative permeability at zero frequency; ω_e, ω_h and ω_κ are the resonant angular frequencies of the permittivity, permeability and chirality, respectively; δ_e, δ_h and δ_κ are the corresponding damping coefficients. τ_k is a characteristic time constant describing the magnitude of chirality.

We define the electric polarization P, P_c and the magnetization M, M_c as follow [24]:

$$\mathbf{P} = \varepsilon_0\chi_e(\omega)\ \mathbf{E} \tag{3a}$$

$$\mathbf{M} = \chi_m(\omega)\ \mathbf{H} \tag{3b}$$

$$\mathbf{P_c} = \chi_c(\omega)\ \mathbf{E} \tag{3c}$$

$$\mathbf{M_c} = \chi_c^*(\omega)\ \mathbf{H} \tag{3d}$$

where χ_e and χ_m are respectively the electric and magnetic susceptibilities, and χ_c is the coupling coefficient:

$$\chi_e(\omega) = \frac{(\varepsilon_s - \varepsilon_\infty)\,\omega_e^2}{\omega_e^2 + j2\delta_e\omega - \omega^2} \tag{4a}$$

$$\chi_m(\omega) = \mu_0\frac{(\mu_s - \mu_\infty)\,\omega_h^2}{\omega_h^2 + j2\delta_h\omega - \omega^2} \tag{4b}$$

$$\chi_c(\omega) = j\frac{\tau_\kappa\,\omega_\kappa^2\,\omega}{c_0(\omega_\kappa^2 + j2\delta_\kappa\omega_\kappa\omega - \omega^2)} \tag{4c}$$

The corresponding electric and magnetic currents are obtained from the time derivatives. In the frequency domain they can be respectively expressed:

$$\mathbf{J_e} = j\omega\mathbf{P} \tag{5a}$$

$$\mathbf{J_m} = j\omega\mathbf{M} \tag{5b}$$

$$\mathbf{J_{ec}} = j\omega\mathbf{P_c} \tag{5c}$$

$$\mathbf{J_{mc}} = j\omega\mathbf{M_c} \tag{5d}$$

By combining Equations (3)–(5) we obtain:

$$(j\omega)^2\,\mathbf{J_e} + (j\omega)2\delta_e\mathbf{J_e} + \omega_e^2\mathbf{J_e} = \varepsilon_0\left(\varepsilon_s - \varepsilon_\infty\right)\omega_e^2(j\omega)\mathbf{E} \tag{6a}$$

$$(j\omega)^2\,\mathbf{J_m} + (j\omega)2\delta_h\mathbf{J_m} + \omega_h^2\mathbf{J_m} = \mu_0\left(\mu_s - \mu_\infty\right)\omega_h^2(j\omega)\mathbf{H} \tag{6b}$$

$$(j\omega)^2\,\mathbf{J_{ec}} + (j\omega)2\omega_\kappa\delta_\kappa\mathbf{J_{ec}} + \omega_\kappa^2\mathbf{J_{ec}} = (j\omega)^2\frac{\tau_\kappa\omega_\kappa^2}{c_0}\mathbf{E} \tag{6c}$$

$$(j\omega)^2\,\mathbf{J_{mc}} + (j\omega)2\omega_\kappa\delta_\kappa\mathbf{J_{mc}} + \omega_\kappa^2\mathbf{J_{mc}} = -(j\omega)^2\frac{\tau_\kappa\omega_\kappa^2}{c_0}\mathbf{H} \tag{6d}$$

In the case of harmonic fields, the set of Equation (6) can be rewritten as:

$$\frac{\partial^2 J_{eu}}{\partial t^2} + 2\delta_e\frac{\partial J_{eu}}{\partial t} + \omega_e^2 J_{eu} = \varepsilon_0\left(\varepsilon_s - \varepsilon_\infty\right)\omega_e^2\frac{\partial E_u}{\partial t} \tag{7a}$$

$$\frac{\partial^2 J_{mu}}{\partial t^2} + 2\delta_h\frac{\partial J_{mu}}{\partial t} + \omega_h^2 J_{mu} = \mu_0\left(\mu_s - \mu_\infty\right)\omega_h^2\frac{\partial H_u}{\partial t} \tag{7b}$$

$$\frac{\partial^2 J_{ecu}}{\partial t^2} + 2\omega_\kappa\delta_\kappa\frac{\partial J_{ecu}}{\partial t} + \omega_\kappa^2 J_{ecu} = \frac{\tau_\kappa\omega_\kappa^2}{c_0}\frac{\partial^2 E_u}{\partial t^2} \tag{7c}$$

$$\frac{\partial^2 J_{mcu}}{\partial t^2} + 2\omega_\kappa\delta_\kappa\frac{\partial J_{mcu}}{\partial t} + \omega_\kappa^2 J_{mcu} = -\frac{\tau_\kappa\omega_\kappa^2}{c_0}\frac{\partial^2 H_u}{\partial t^2} \tag{7d}$$

with $u \in \{x, y, z\}$.

The discretization of the set of Equation (7) allows us to write:

$$J_{eu}^{n+\frac{3}{2}} = \alpha_e\,J_{eu}^{n+\frac{1}{2}} + \beta_e\,J_{eu}^{n-\frac{1}{2}} + \gamma_e\left({}_{n+1}V_u - {}_{n-1}V_u\right) \tag{8a}$$

$$J_{mu}^{n+1} = \alpha_h\,J_{mu}^{n} + \beta_h\,J_{mu}^{n-1} + \gamma_h\left({}_{n+\frac{1}{2}}I_u - {}_{n-\frac{3}{2}}I_u\right) \tag{8b}$$

$$J_{ecu}^{n+\frac{3}{2}} = \alpha_c\,J_{ecu}^{n+\frac{1}{2}} + \beta_c\,J_{ecu}^{n-\frac{1}{2}} + \gamma_c\left({}_{n+2}V_u - 2\,{}_{n+1}V_u + {}_{n}V_u\right) \tag{8c}$$

$$J_{mcu}^{n+1} = \alpha_c\,J_{mcu}^{n} + \beta_c\,J_{mcu}^{n-1} - \gamma_c\left({}_{n+\frac{3}{2}}I_u - 2{}_{n+\frac{1}{2}}I_u + {}_{n-\frac{1}{2}}I_u\right) \tag{8d}$$

with:

$$\alpha_e = \frac{2-\omega_e^2\Delta t^2}{1+\delta_e\Delta t},\quad \beta_e = \frac{\delta_e\Delta t - 1}{1+\delta_e\Delta t},\quad \gamma_e = \frac{\varepsilon_0\left(\varepsilon_s-\varepsilon_\infty\right)\omega_e^2\Delta t}{2\left(1+\delta_e\Delta t\right)\Delta l}, \tag{9a}$$

$$\alpha_h = \frac{2-\omega_h^2\Delta t^2}{1+\delta_h\Delta t},\quad \beta_h = \frac{\delta_h\Delta t - 1}{1+\delta_h\Delta t},\quad \gamma_h = \frac{\mu_0\left(\mu_s-\mu_\infty\right)\omega_h^2\Delta t}{2\left(1+\delta_h\Delta t\right)\Delta l}, \tag{9b}$$

$$\alpha_c = \frac{2-\omega_\kappa^2\Delta t^2}{1+\omega_\kappa\delta_\kappa\Delta t},\quad \beta_c = \frac{\omega_\kappa\delta_\kappa\Delta t - 1}{1+\omega_\kappa\delta_\kappa\Delta t},\quad \gamma_c = \frac{\tau_\kappa\omega_\kappa^2}{c_0\left(1+\omega_\kappa\delta_\kappa\Delta t\right)\Delta l} \tag{9c}$$

where the analogies between electromagnetic field components and pulses on transmission lines for a uniform TLM mesh are used [25]:

$$E_u^n = \frac{{}_nV_u}{\Delta l} \quad \text{and} \quad H_u^{n+\frac{1}{2}} = \frac{{}_{n+\frac{1}{2}}I_u}{\Delta l} \tag{10}$$

${}_nV_u$ and ${}_{n+\frac{1}{2}}I_u$ are respectively the total voltage at the time step $n\Delta t$ and the total current at the time step $(n+\frac{1}{2})\Delta t$ in the u direction, and Δl is the length of the uniform cubical TLM cell.

In the case of the traditional SCN, the requirement that all link lines have the same characteristic impedances equal to the intrinsic impedance of free-space ($Z_0 = \sqrt{(\mu_0\epsilon_0)}$) implies that the SCN models the background medium (the free space in this case). In order to accommodate the SCN and electromagnetic parameters of chiral medium, stubs are loaded into the TLM nodes. So, as it appears in Figures 1(a), (b), three open-circuit stubs (one for each direction) and three short-circuit stubs are used to account for, respectively, extra capacitance and inductance [25]. The dispersive behaviour can be incorporated in the TLM model in a similar manner, by introducing additional stubs. So three stubs

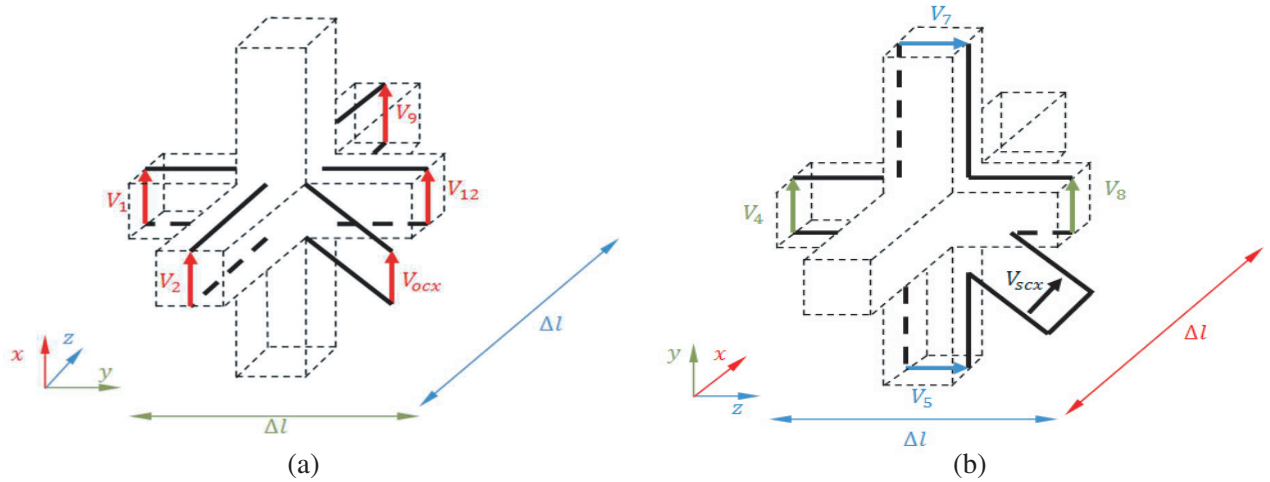

Figure 1. SCN loaded with (a) capacitive stub in the x direction, (b) inductive stub in the x direction.

are added to the loaded SCN (one for each direction of the space) and are considered as voltage sources, and three other stubs are added to the node and are considered as current sources.

In order to obtain the expression of the 12 stubs, we use a comparison between discritized Maxwell equations of the chiral medium and the discretized SCN loaded stubs mesh equations.

According to Equation (1) we have:

$$\boldsymbol{\nabla} \times \mathbf{H} = j\omega\varepsilon_0\varepsilon_\infty \mathbf{E} + j\omega\,\varepsilon_0\chi_e \mathbf{E} - j\omega\chi_c\,\mathbf{H} \tag{11a}$$

$$\boldsymbol{\nabla} \times \mathbf{E} = -j\omega\mu_0\mu_\infty \mathbf{H} - j\omega\,\mu_0\chi_m \mathbf{H} - j\omega\chi_c\,\mathbf{E} \tag{11b}$$

Substituting Equations (3)–(5) into Equation (11), we get:

$$\boldsymbol{\nabla} \times \mathbf{H} = \varepsilon_0\varepsilon_\infty \frac{\partial \mathbf{E}}{\partial t} + \mathbf{J_e} + \mathbf{J_{mc}} \tag{12a}$$

$$\boldsymbol{\nabla} \times \mathbf{E} = -\mu_0\mu_\infty \frac{\partial \mathbf{H}}{\partial t} - \mathbf{J_m} - \mathbf{J_{ec}} \tag{12b}$$

The discretization of Equation (12) allows us to write:

$${}_{n+1}V_u = {}_nV_u + \frac{\Delta l \Delta t}{\varepsilon_0\varepsilon_\infty}\left[(\boldsymbol{\nabla} \times \mathbf{H})_u^{n+\frac{1}{2}} - \left(J_{eu}^{n+\frac{1}{2}} + J_{mcu}^{n}\right)\right] \tag{13a}$$

$${}_{n+1}I_u = {}_nI_u - \frac{\Delta l \Delta t}{\mu_0\mu_\infty}\left[(\boldsymbol{\nabla} \times \mathbf{E})_u^{n+\frac{1}{2}} + \left(J_{mu}^{n+\frac{1}{2}} + J_{ecu}^{n}\right)\right] \tag{13b}$$

The followed approach for calculating node parameters in TLM schemes is based on equating total capacitance and inductance contributed by the link and stub lines of a TLM cell to the corresponding parameters of the block of modelled medium [25]. The equivalent total voltage V_u is derived by combining conditions for charge balance and charge conservation for the transmission-lines coupling with E_u field component, while the equivalent total current I_u is derived by combining conditions for magnetic flux balance and conservation for the transmission-lines coupling with H_u field component. The resulting voltage and current at each node can be expressed as:

$${}_{n+1}\begin{pmatrix} V_x \\ V_y \\ V_z \end{pmatrix} = \begin{pmatrix} \dfrac{2}{4+\hat{Y}_{ocx}} \\ \dfrac{2}{4+\hat{Y}_{ocy}} \\ \dfrac{2}{4+\hat{Y}_{ocz}} \end{pmatrix} \cdot \begin{pmatrix} {}_{n+1}V_1^i + {}_{n+1}V_2^i + {}_{n+1}V_9^i + {}_{n+1}V_{12}^i + \hat{Y}_{ocx}V_{ocx}^i + 0.5\ {}_{n+1}V_{sx} \\ {}_{n+1}V_3^i + {}_{n+1}V_4^i + {}_{n+1}V_8^i + {}_{n+1}V_{11}^i + \hat{Y}_{ocy}V_{ocy}^i + 0.5\ {}_{n+1}V_{sy} \\ {}_{n+1}V_5^i + {}_{n+1}V_6^i + {}_{n+1}V_7^i + {}_{n+1}V_{10}^i + \hat{Y}_{ocz}V_{ocz}^i + 0.5\ {}_{n+1}V_{sz} \end{pmatrix} \tag{14a}$$

$$ {}_{n+1}\begin{pmatrix} I_x \\ I_y \\ I_z \end{pmatrix} = \begin{pmatrix} \dfrac{2}{4+\hat{Z}_{scx}} \\ \dfrac{2}{4+\hat{Z}_{scy}} \\ \dfrac{2}{4+\hat{Z}_{scz}} \end{pmatrix} \cdot \begin{pmatrix} {}_{n+1}I^i_7 - {}_{n+1}I^i_5 + {}_{n+1}I^i_4 - {}_{n+1}I^i_8 - I^i_{scx} + 0.5\ {}_{n+1}I_{sx} \\ {}_{n+1}I^i_9 - {}_{n+1}I^i_2 + {}_{n+1}I^i_6 - {}_{n+1}I^i_{10} - I^i_{scy} + 0.5\ {}_{n+1}I_{sy} \\ {}_{n+1}I^i_{11} - {}_{n+1}I^i_3 + {}_{n+1}I^i_1 - {}_{n+1}I^i_{12} - I^i_{scz} + 0.5\ {}_{n+1}I_{sz} \end{pmatrix} \quad (14b) $$

where $\hat{Y}_{ocu}$ and $\hat{Z}_{scu}$ are respectively the normalized admittance of the open circuit capacitive stub and the normalized impedance of the short circuit inductive stub in the u direction; V^i_{ocu} is the incident voltage on the open circuit stub; I^i_{scu} is the incident current on the short circuit stub; ${}_{n+1}V_{su}$ and ${}_{n+1}I_{su}$ are respectively the voltage and current sources at the time step $(n+1)\Delta t$.

Then, the use of the expression of EM field components in function of incident and reflected pulses so as to obtain the equivalent voltages and currents in the node at the time step $(n+1)\Delta t$ [26] gives us:

$$ {}_{n+1}V_u = {}_nV_u + \frac{1}{4+\hat{Y}_{ocu}}\left({}_{n+1}V_{su} + {}_nV_{su}\right) + \frac{4}{4+\hat{Y}_{ocu}}\frac{\Delta l \Delta t}{\varepsilon_0}\left(\nabla \times H\right)^{n+\frac{1}{2}}_u \quad (15a) $$

$$ {}_{n+1}I_u = {}_nI_u + \frac{1}{4+\hat{Z}_{scu}}\left({}_{n+1}I_{su} + {}_nI_{su}\right) - \frac{4}{4+\hat{Z}_{scu}}\frac{\Delta l \Delta t}{\mu_0}\left(\nabla \times E\right)^{n+\frac{1}{2}}_u \quad (15b) $$

The analogy between the sets of Equations (13) and (15) allows us to obtain the update expression of the voltage and current sources:

$$ {}_{n+1}V_{su} = -{}_nV_{su} - 4\frac{\Delta l \Delta t}{\varepsilon_0}\left(J^{n+\frac{1}{2}}_{eu} + J^n_{mcu}\right) \quad (16a) $$

$$ {}_{n+1}I_{su} = -{}_nI_{su} - 4\frac{\Delta l \Delta t}{\mu_0}\left(J^{n+\frac{1}{2}}_{mu} + J^n_{ecu}\right) \quad (16b) $$

and the expression of the admittance and the impedance of capacitive and inductive stubs:

$$ \hat{Y}_{ocu} = 4\left(\varepsilon_\infty - 1\right) \quad (17a) $$

$$ \hat{Z}_{scu} = 4\left(\mu_\infty - 1\right) \quad (17b) $$

3. VALIDATION OF THE ADE-TLM MODEL FOR CHIRAL MEDIA

In order to verify the validity and accuracy of the TLM model proposed above for the chiral media, the interaction of an EM wave in normal incidence with a chiral slab is simulated. The structure used is subdivided into 400 cells, each with thickness 75 µm. The chiral medium occupies cells 101 to 300 while the free space occupies cells 1 to 100 and 301 to 400. The chiral medium in the structure has the following parameters: $\epsilon_s = 4.4$, $\epsilon_\infty = 3.5$, $\mu_s = 1.1$, $\mu_\infty = 1$, $\omega_e = \omega_h = \omega_k = 16\pi$ GHz, $\delta_e = \delta_h = 0.07\omega_e$, $\delta_k = 0.09$ and $\tau_k = 1$ ps.

Figure 2 illustrates the real and imaginary parts of the relative permittivity, relative permeability and chirality for the chiral medium used in the simulation. As can be seen, the resonant frequency is equal to 8 GHz.

The structure is excited by a differential Gaussian pulse of expression in the time domain: $E_i(t) = \frac{(t-t_0)}{\tau}\exp\left(-\frac{4\pi(t-t_0)^2}{\tau^2}\right)$, with $t_0 = 120\Delta t$ and $\tau = 150\Delta t$. The excitation is introduced at the 10th cell, and the simulations are programmed to effect 20,000 iterations. The co-polarized and cross-polarized transmission and reflection coefficients are computed numerically by the ADE-TLM approach and compared to the exact results [27].

The time domain response of the co-polarized and cross-polarized reflected and transmitted waves computed using the ADE-TLM method introduced in this paper are shown in Fig. 3. Since the incident wave is polarized in the x direction, the appearance of the y component in the transmitted wave proves the ability of chiral medium to rotate the incident wave polarization plane. In order to visualize the influence of the chirality parameter on the optical activity, we have made numerical validation experiment. As the characteristic time constant describes the chirality magnitude, we have chosen

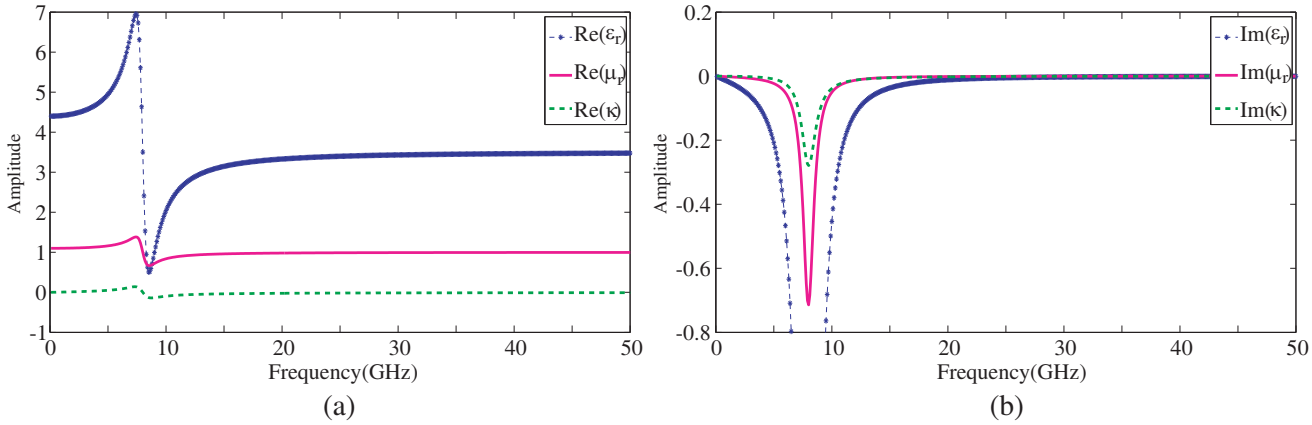

Figure 2. Relative permittivity, permeability and chirality of the chiral medium used in the simulation. (a) Real part. (b) Imaginary part.

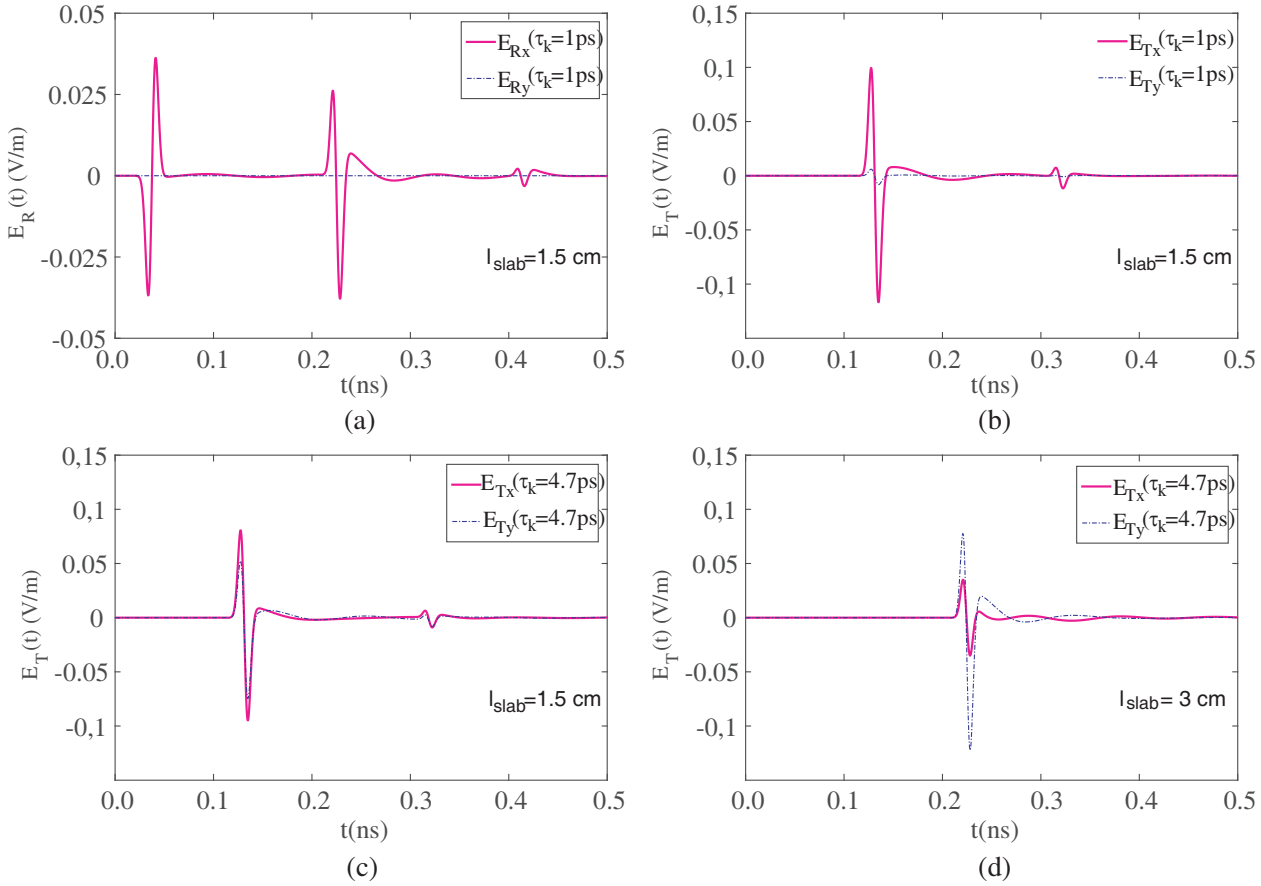

Figure 3. Co-polarized and cross polarized of reflected and transmitted wave. (a) Reflected wave. (b) Transmitted wave. (c) Transmitted wave. (d) Transmitted wave.

two values of $\tau_k = 1\,\text{ps}$ and $\tau_k = 4.7\,\text{ps}$ for the characteristic time constant; the other parameters of the medium and the excitation are kept the same as in the previous simulation. The results of this numerical experiment are presented in Figs. 3(b) and 3(c). Comparison between these figures shows that the optical activity is proportional to the characteristic time constant. An additional numerical experiment is performed with chiral medium occupying cells 101 to 500 to visualize the influence of the

slab thickness on the optical activity. Result is presented in Fig. 3(d). It can be observed from Figs. 3(c) and 3(d) that the amount of rotation in the plane of polarization is proportional to the thickness of the medium traversed by the wave.

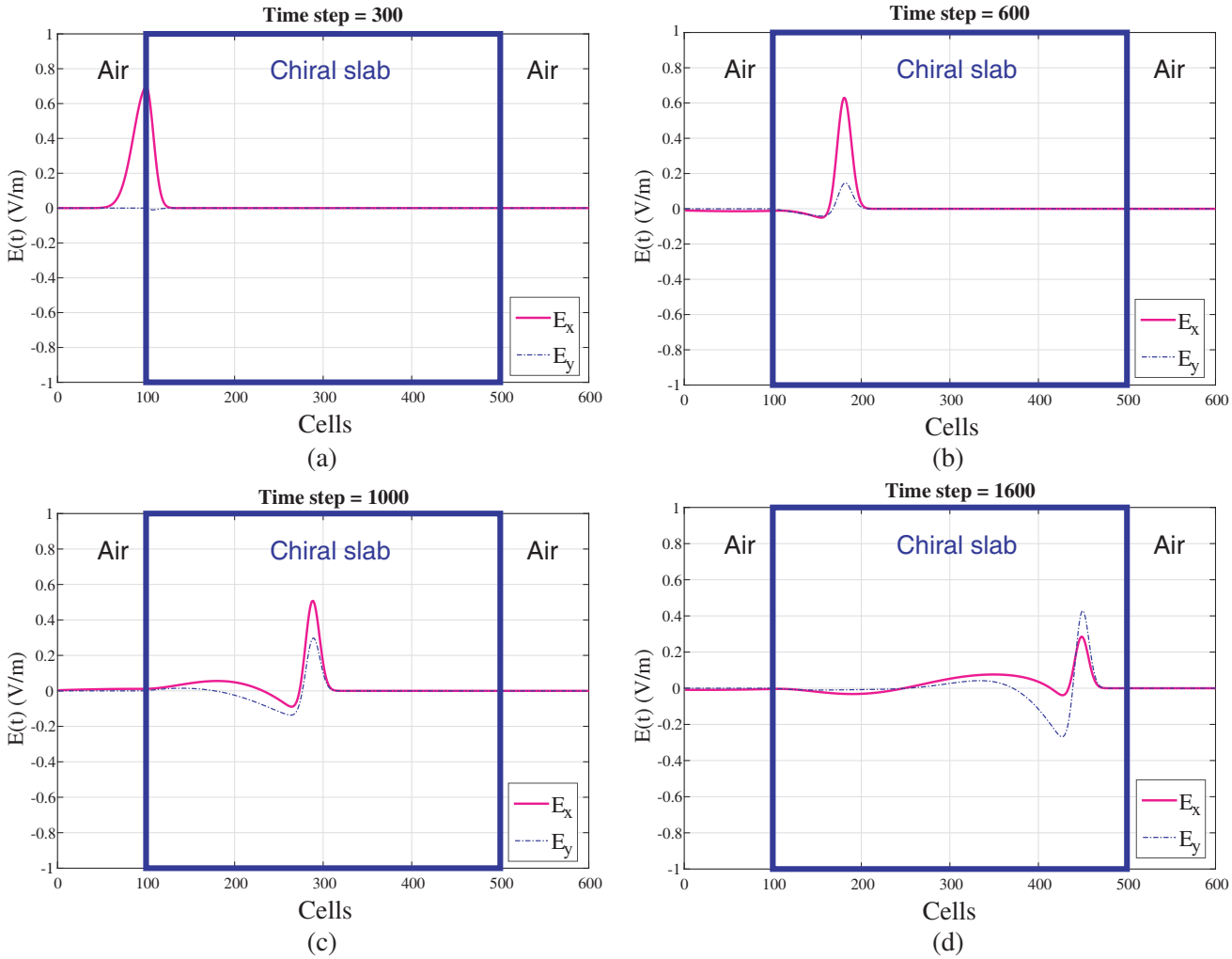

Figure 4. Propagation of co- and cross-polarized fields.

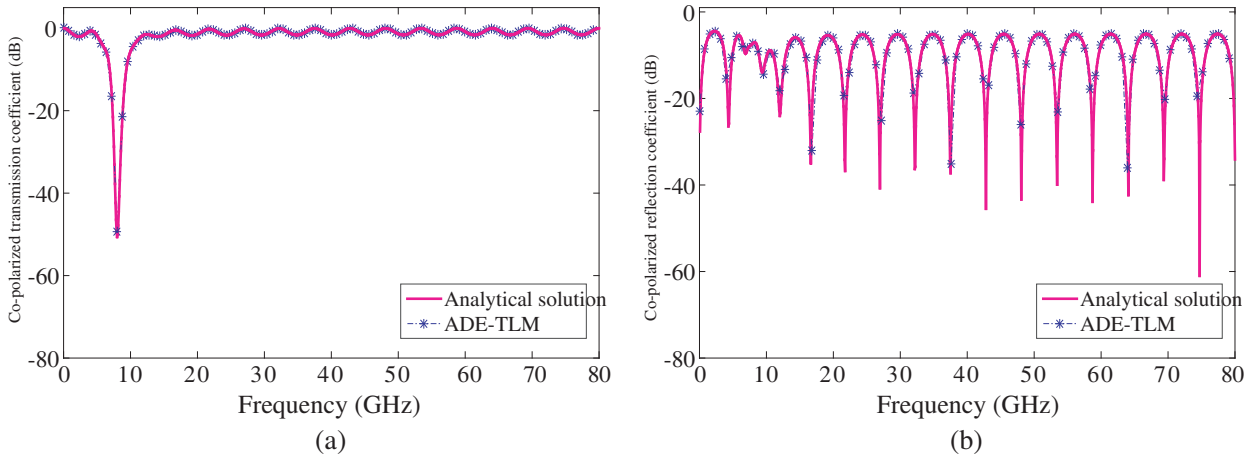

Figure 5. (a) Co polarized transmission coefficient, (b) co polarized reflection coefficient.

The developed dispersive chiral TLM formulation is used to visualize how the co- and cross-polarized fields propagate through the chiral media in the time domain. A chiral slab of thickness 3 cm is illuminated by a Gaussian waveform of expression $E_i(t) = \exp\left(-\frac{4\pi(t-t_0)^2}{\tau^2}\right)$, with $t_0 = 120\Delta t$ and $\tau = 150\Delta t$. The medium parameters are the same as in the previous simulation with $\tau_k = 4.5$ ps. Results are presented in Fig. 4. It is clearly visible that cross-polarized field is generated as the Gaussian wave propagates through the chiral slab. Transmitted field has a cross-polarized component while reflected field does not. The amplitude of the cross polarized component increases as the wave travels in the z-direction through the chiral domain, while the co-polarized component amplitude decreases.

Figures 5–6 show the magnitudes of co-polarized and cross-polarized reflection and transmission coefficients in frequency domain computed using the ADE-TLM method introduced in this paper and the analytical method. From these figures, we can observe that the ADE-TLM simulation results are in excellent agreement with their analytical counterparts at all frequencies.

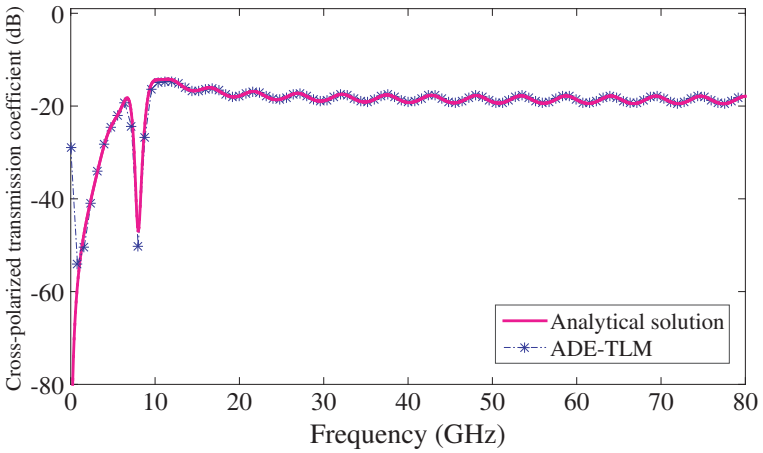

Figure 6. Cross-polarized transmission coefficient.

4. CONCLUSION

In this paper, a TLM based method for modelling wave interaction with chiral medium is derived using auxiliary differential equations. To illustrate the efficiency and accuracy of this method, co-polarized and cross-polarized reflection and transmission coefficients in frequency domain through a chiral material are computed and compared to the analytical ones. Results demonstrate excellent agreement between the proposed algorithm and analytical scheme. Additional numerical experiment is performed in order to visualize the effect of polarization rotation due to the chirality parameter and medium thickness.

REFERENCES

1. Cheng, Y. Z., Y. Nie, Z. Z. Cheng, X. Wang, and R. Z. Gong, "Asymmetric chiral metamaterial circular polarizer based on twisted split-ring resonator," *Appl. Phys. B*, Vol. 116, No. 1, 129–134, 2014.
2. Zebiri, C. and F. Benabdelaziz, "Asymptotic approach for rectangular microstrip patch antenna with magnetic anisotropy and chiral substrate," *World Academy of Science, Engineering and Technology*, Vol. 2, 316–322, 2008.
3. Guven, K., E. Saenz, R. Gonzalo, et al., "Electromagnetic cloaking with canonical spiral inclusions," *New J. Phys.*, Vol. 10, No. 11, 2008.
4. Li, M., L. Guo, J. Dong, and H. Yang, "An ultra-thin chiral metamaterial absorber with high selectivity for LCP and RCP waves," *Journal of Physics D: Applied Physics*, Vol. 47, 2014.

5. Tretyakov, S. A. and A. A. Sochava, "Proposed composite material for nonreflecting shields and antenna radomes," *Electronics Letters*, Vol. 29, No. 12, 1048–1049, 1993.
6. Prosvirnin, S. L. and N. I. Zheludev, "Analysis of polarization transformations by a planar chiral array of complex-shaped particles," *Journal of Optics A: Pure and Applied Optics*, Vol. 11, 2009.
7. Varadan, V. K., A. Lkhtakia, and V. V. Varadan, "Propagation in a parallel-plate waveguide wholly filled with a chiral medium," *Journal of Wave-material Interaction*, Vol. 3, No. 3, 267–272, 1988.
8. Grande, A., I. Barba, A. C. L. Cabeceira, J. Represa, P. P. M. So, and W. J. R. Hoefer, "FDTD modeling of transient microwave signals in dispersive and lossy bi-isotropic media," *IEEE Transactions on Microwave Theory and Techniques*, Vol. 52, No. 3, 773–783, 2004.
9. Akyurtlu, A., D. H. Werner, and K. Aydin, "Bi-FDTD: A new technique for modeling electromagnetic wave interaction with Bi-isotropic media," *Microwave and Optical Technology Letters*, Vol. 26, No. 4, 239–242, 2000.
10. Akyurtlu, A., D. H. Werner, and K. Aydin, "A novel FDTD technique for modeling chiral media," *IEEE Antennas Propagation Society Int. Symp.*, Vol. 3, 1332–1335, Salt Lake City, UT, 2000,
11. Akyurtlu, A. and D. H. Werner, "Modeling chiral media using a new dispersive FDTD technique,", *IEEE Antennas Propagation Society Int. Symp.*, Vol. 1, 44–47, Boston, MA, 2001,
12. Akyurtlu, A. and D. H. Werner, "Analysis of double negative media with magneto-electric coupling using a novel dispersive FDTD formulation," *IEEE Int. Symp. Antennas Propagation USNC/URSI Nat. Radio Science Meeting*, Vol. 3, 371–374, Columbus, 2003.
13. Akyurtlu, A. and D. H. Werner, "BI-FDTD: A novel finite-difference time-domain formulation for modeling wave propagation in bi-isotropic media," *IEEE Transactions on Antennas and Propagation*, Vol. 52, No. 2, 416–425, 2004.
14. Akyurtlu, A. and D. H. Werner, "A Novel dispersive FDTD formulation for modeling transient propagation in chiral metamaterials," *IEEE Transactions on Antennas and Propagation*, Vol. 52, No. 9, 2267–2276, 2004.
15. Demir, V., A. Z. Elsherbeni, and E. Arvas, "FDTD formulation for dispersive chiral media using the z transform method," *IEEE Transactions on Antennas and Propagation*, Vol. 53, No. 10, 3374–3384, 2005.
16. Attiya, A. M., "Shift-operator finite difference time domain analysis of chiral medium," *Progress In Electromagnetics Research M*, Vol. 13, 29–40, 2010.
17. Grande, A., I. Barba, A. C. L. Cabeceira, J. Represa, K. Karkkainen, and A. H. Sihvola, "Two-Dimensional Extension of a Novel FDTD technique for modeling dispersive lossy bi-isotropic media using the auxiliary differential equation method," *IEEE Microwave and Wireless Components Letters*, Vol. 15, No. 5, 375–377, 2005.
18. Wang, M. Y., H. F. Mu, W. Chen, L. Zhao, and J. Xu, "FDTD analysis of chiral metamaterials slab by using the auxiliary differential equation algorithm," *Frequenz*, Vol. 67, No. 5–6, 155–161, DE Gruyter, 2013.
19. Pereda, J. A., A. Grande, O. Gonzalez, and A. Vegas, "FDTD modeling of chiral media by using the mobius transformation technique," *IEEE Antennas and Wireless Propagation Letters*, Vol. 5, 327–330, 2006.
20. Paul, J., C. Christopoulos, and D. W. P. Thomas, "Time-domain modeling of electromagnetic wave propagation in complex materials," *Electromagnetics*, Vol. 19, No. 6, 527–546, 1999.
21. Yaich, M. I., M. Khalladi, and M. Essaaidi, "Efficient modeling of chiral media using SCN-TLM method," *Serbian Journal of Electrical Engineering*, 249–254, 2004.
22. Cabeceira, C. L., A. Grande, I. Barba, and J. Represa, "A 2D-TLM model for electromagnetic wave propagation in chiral media," *Antennas & Propagation Society International Symposium*, Vol. 2, No. 5, 1487–1490, 2004.
23. Sihvola, A. H., "Electromagnetic modeling of bi-isotropic media," *Progress In Electromagnetic Research*, Vol. 9, 45–86, 1994.
24. Solymar, L., *Electrical Properties of Materials*, Oxford University Press Inc., New York, 2010.

25. Christopoulos, C., "The Transmission-Line Modeling (TLM) method in electromagnetics," *Synthesis Lectures on Computational Electromagnetics*, Morgan & Claypool, 2006.
26. Jin, H. and R. Vahldieck, "Direct derivation of the TLM symmetrical condensed node and hybrid symmetrical condensed node from Maxwell's equations using centered differencing and averaging," *IEEE Transactions on Microwave Theory and Techniques*, Vol. 42, 2554–2561, Dec. 1994.
27. Zhao, R., T. Koschny, and C. M. Soukoulis, "Chiral metamaterials: Retrieval of the effective parameters with and without substrate," *Optics Express*, Vol. 18, No. 14, 14553–14567, Jul. 2010.